

A small aperture enabling the encapsulation of HF in [60]fullerene

Shumpei Sadai, Yoshifumi Hashikawa* and Yasujiro Murata*

Institute for Chemical Research, Kyoto University: Gokasho, Uji, Kyoto 611–0011, Japan

A small aperture, allowing the encapsulation of hydrofluoric acid (HF), was made in [60]fullerene. To create this structure, reductive decarbonylation was performed on an open [60]fullerene with a 13-atom ring aperture, resulting in two primary derivatives with 14-atom apertures. The chemical structure of the aperture was found to be critical in determining the selectivity between the two derivatives. Despite the reaction being performed at 180 °C in the presence of water, the products spontaneously allowed a water molecule to pass through the aperture. However, under milder conditions at 0 °C, HF was encapsulated in the cavity. The encapsulation of HF led to a distinct shifting of proton signals attributed to the translational movement of HF in the cavity, as predicted by theoretical calculations.

KEYWORDS : Aperture, Capsulation, Fullerene, Hydrogen fluoride

1. Introduction

Fullerene C₆₀ is a spherical carbon cluster consisting of pentagons and hexagons. Successive bond scissions can create apertures in C₆₀ [1–5], and the resulting derivatives can encapsulate specific guests. In 2001, Rubin, Houk, Saunders, Cross, and coworkers reported the creation of a 14-membered-ring aperture on C₆₀ [6]. They also demonstrated guest insertion of ³He and H₂ under harsh conditions, with occupancy levels reaching only 1.5% (288–305 °C, approximately 475 atm, 7.5 h) and 5% (400 °C, 100 atm, 48 h), respectively [7]. It is important to note that smaller apertures may prevent guest molecule encapsulation, while larger apertures may lead to guest release after encapsulation. Additionally, restoring the opened form to pristine C₆₀ can be challenging with larger apertures. To overcome these issues, it is crucial to develop ideal [60]fullerene hosts with apertures that are as small as possible to facilitate efficient encapsulation of various guests.

In 2011, we reported a cage-opened C₆₀ derivative with a 13-membered-ring aperture [8, 9]. Under 9,000 atm at 120 °C for 36 h, water was quantitatively encapsulated. During this process, the aperture of the host transformed in situ into a 16-membered ring, creating a window through which a water molecule passed before returning to the original 13-membered-ring orifice. However, under ambient pressure at 160 °C for 24 h, the encapsulation ratio of water was less than 10% [10, 11]. Related C₆₀ derivatives with a 16-membered-ring aperture encapsulate water molecules at an occupancy level of approximately

5% under ambient pressure at 180 °C for 15 min [12]. The first cage-opened C₆₀ derivative, reported by Wudl and coworkers in 1995, has an 11-membered-ring aperture that prevents the encapsulation of any chemical species [13]. Using this compound, we synthesized an orifice-expanded derivative with a 12-membered-ring aperture, resulting in 33% H₂ encapsulation under 165 atm at 150 °C for 24 h. In this process, the actual encapsulation window is an in situ-generated 15-membered ring [14, 15]. As exemplified above, high-pressure conditions are typically necessary for encapsulation with a reasonable guest occupancy level. Recently, we reported a small 14-membered-ring aperture that enables a high water-encapsulation ratio of 78% at 180 °C for 24 h without applying high pressure [16]. However, undesired side reactions occurred during the synthetic preparation of the aperture, generating additional products and lowering the yield of the desired 14-membered ring. This is attributed to a reactive imine moiety on an orifice of the precursor molecule. To address this issue, a precursor molecule without the imine moiety is required. Herein, we report an improved synthesis of the small 14-membered-ring aperture for guest insertion by replacing the imine with an olefin in the precursor molecule. We also discuss the spontaneous encapsulation of HF inside the C₆₀ host under milder conditions, as well as the translational motion of HF in the cavity (**Fig. 1**).

2. Results and Discussion

In our previous report [16], **1a**, which bears an imine moiety on its

* Corresponding Authors, E-mail: hashi@scl.kyoto-u.ac.jp,
yasujiro@scl.kyoto-u.ac.jp

<https://doi.org/10.7209/carbon.040106>



(Received November 26, 2024, Accepted December 19, 2024)

(J-STAGE Advance published December 27, 2024)

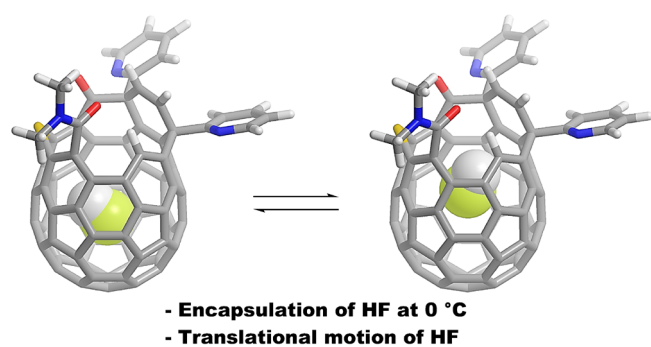


Fig. 1 HF encapsulation through a small aperture.

aperture, could be transformed into **2a**, **3a**, and **4a** in isolated yields of 35%, 3%, and 39%, respectively, through a reaction assisted by a single-electron reductant, namely, tris(dimethylamino)methane (TDAM, $\text{CH}(\text{NMe}_2)_3$) in a mixed solvent media of *o*-dichlorobenzene (ODCB) and water at 180 °C for 24 h (**Fig. 2a**). Notably, all three products spontaneously accommodate a water molecule inside with occupancy levels of 32%, 78%, and 32%, respectively. The water contents were determined by comparing the signal areas in ^1H NMR spectra. All these compounds were characterized spectroscopically and/or crystallographically in the previous work [16].

Similarly, we performed the reaction using **1b**, yielding $\text{H}_2\text{O}@2\text{b}$ and $\text{H}_2\text{O}@3\text{b}$ in 4% and 68% yields, respectively. Notably, **4b** was not generated because the olefin moiety in **1b** did not undergo hydrolysis, unlike the reaction of **1a**, which partially yielded the hydrolyzed product (**4a**). The encapsulation ratios of $\text{H}_2\text{O}@2\text{b}$ and $\text{H}_2\text{O}@3\text{b}$ were determined to be 22% and 39%, respectively. Structural characterization was performed using mass spectrometry and NMR spectroscopy. Mass spectrometric analysis of $\text{H}_2\text{O}@2\text{b}$ clearly showed the expected decarbonylation of **1b**, with a molecular ion peak detected at m/z 982.0761, assignable to $[\text{1b}-\text{CO}+2\text{H}+\text{H}_2\text{O}]^+$ (**Fig. S3**). The ^{13}C NMR spectrum of $\text{H}_2\text{O}@2\text{b}$ confirmed the disappearance of one carbonyl signal (**Fig. S2**). In the ^1H NMR spectrum (800 MHz, acetone- d_6 /CS $_2$ (1 : 5)), two new singlet signals emerged in the aromatic region at δ 8.86 and 8.78 ppm (**Fig. S1**). Notably, these proton signals are shifted downfield even compared to the electron-deficient protons of the pyridyl substituents (8.52 and 8.48 ppm). This indicates that these protons are directly attached to the electron-deficient [60]fullerene cage, resulting in a considerable deshielding effect. The molecular ion peak of $\text{H}_2\text{O}@3\text{b}$ was identified at m/z 1053.1149, which corresponds to $[\text{1b}+\text{NHMe}_2+\text{H}_2\text{O}]^+$ (**Fig. S7**). Multiple long-range $^1\text{H}-^{13}\text{C}$ correlations, such as NMe_2 (δ 3.40 and 2.88 ppm) \cdots $\text{C}=\text{O}$ (δ 166.19 ppm) and CH (δ 9.89 ppm) \cdots CPy (δ 54.07 ppm), confirm the presence of an amide group and an aromatic proton attached to the fullerene cage (**Fig. S6**). These correlation peaks also reveal the substitution site of the amide group.

This chemical transformation begins with the nucleophilic addition of water to one of the two carbonyl groups in **1**, resulting in the

formation of the geminal diol **INT1**. Subsequently, **INT1** undergoes C–C bond cleavage to potentially generate **INT2** and **INT3** (**Fig. 2a**). TDAM is believed to play a role in facilitating the C–C bond cleavage process [16]. By comparing the structures, **3** can be deduced to be derived from **INT3** via further reaction with HNMe_2 , which is generated in situ from TDAM (**Fig. 2b**). Meanwhile, **2** could be formed from either **INT2** or **INT3**, concomitant with the release of CO_2 . Lastly, **4** is proposed to arise from **INT2** through hydrolysis of the imine moiety, followed by condensation and release of benzoic acid [16]. Upon examining the encapsulation ratios of H_2O , the same value of 32% was observed for both $\text{H}_2\text{O}@2\text{a}$ and $\text{H}_2\text{O}@4\text{a}$ despite their structurally distinct apertures. To gain insights into the water-encapsulation process, we calculated the insertion barriers of H_2O at the B3LYP-D3/6-31G(d) level of theory (**Fig. 2a**). The calculations revealed that the insertion barrier for **2a** was estimated to be $\Delta G^\ddagger +26.6$ kcal/mol, which is considerably lower than that for **4a** (+36.9 kcal/mol). However, this result does not fully explain the comparable water contents in $\text{H}_2\text{O}@2\text{a}$ and $\text{H}_2\text{O}@4\text{a}$. Additionally, the high activation barrier of $\Delta G^\ddagger +36.9$ kcal/mol for **4a** makes it unlikely that the process would proceed at 180 °C. However, the intermediate of **2a** and **4a** (namely, **INT2a**) is predicted to undergo water encapsulation with an activation barrier of +17.4 kcal/mol. Therefore, water insertion likely occurs on **INT2a** before the formation of **2a** and **4a**, resulting in the same water occupation ratio. This further supports the notion that **2a** is predominantly generated from **INT2a**. In contrast, the water occupation ratio for $\text{H}_2\text{O}@3\text{a}$ should be determined after the generation of **3a** because the activation barrier for **3a** is estimated to be +21.5 kcal/mol, which is $\Delta\Delta G^\ddagger -2.1$ kcal/mol lower than that of its intermediate (**INT3a**, +23.6 kcal/mol).

In the case of the olefin analog, the water insertion process for **2b** is similar to that for **2a**. The activation barrier for **2b** (+28.8 kcal/mol) is predicted to be higher than that of **INT2b** (+20.2 kcal/mol), suggesting that water insertion occurs before the conversion of **INT2b** into **2b**. A similar water insertion process is also proposed for $\text{H}_2\text{O}@3\text{b}$, where its barrier of +26.5 kcal/mol is higher than that of **INT3b** (+24.9 kcal/mol). This process differs from that of $\text{H}_2\text{O}@3\text{a}$, whose occupation level is determined after its generation.

It is noteworthy that changing the substructure of the aperture from imine functionality to olefin reverses the selectivity between **INT2** and **INT3** (**3a** or **3b**). In the case of the imine analogs, **3a**, derived from **INT3a**, was obtained as the minor product in 3% yield, while the combined yield of **2a** and **4a** (both from **INT2a**) was 74%. Conversely, for the olefin analog, **3b** (from **INT3b**) was obtained in 68% yield, while **2b** (from **INT2b**) was the minor product in 4% yield. The preferred formation of **INT2a** over **INT3a** is likely attributed to the stabilization of the transition state by an intramolecular hydrogen bond between the carboxylic acid and the imine moiety. In the olefin analog, however, there is no such assistance for the formation

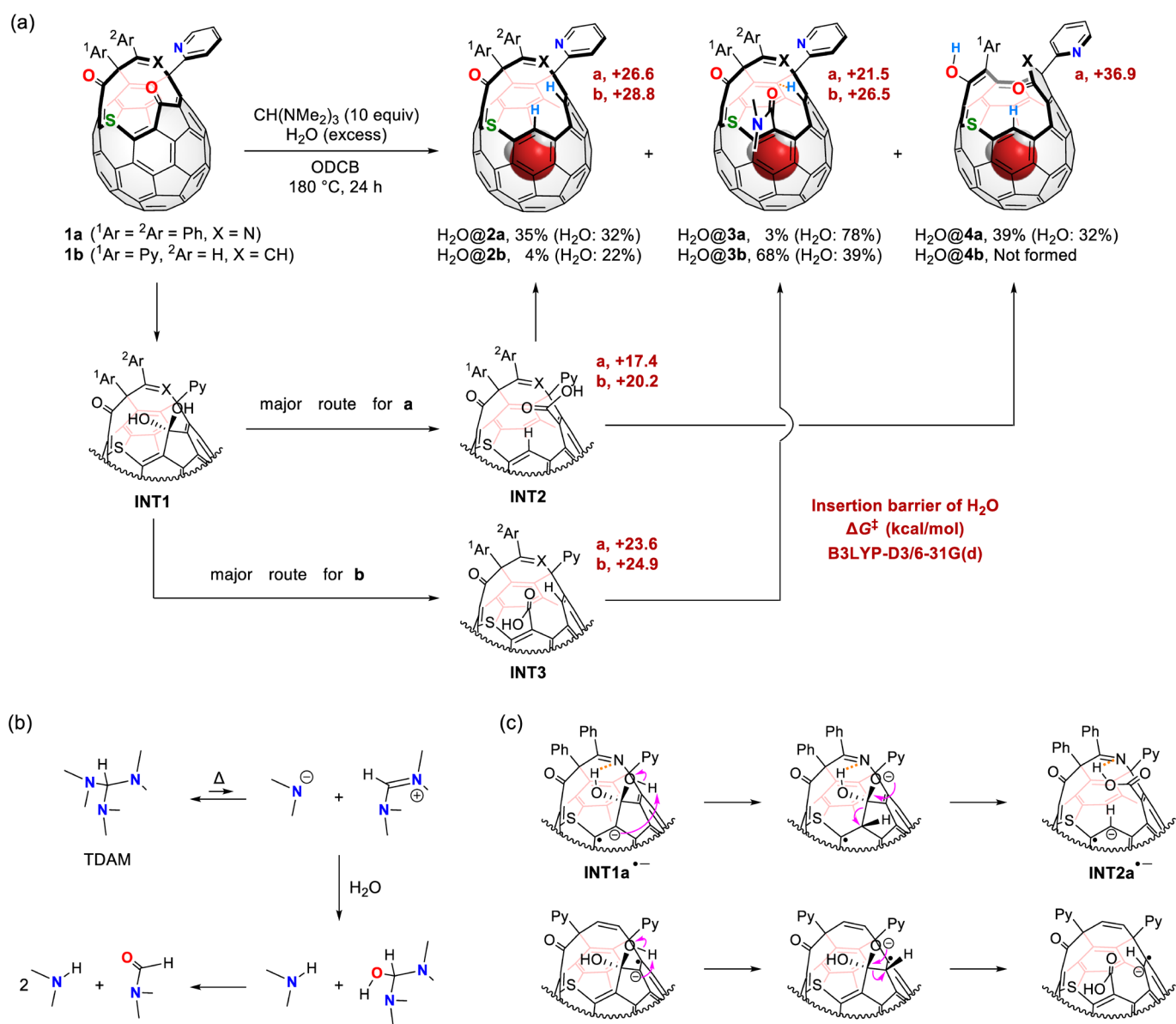


Fig. 2 (a) Synthesis and reaction pathways with insertion barriers of H₂O, ΔG[‡] (kcal/mol) at 298 K, calculated at the B3LYP-D3/6-31G(d) level of theory. (b) Proposed mechanism for the generation of Me₂NH. (c) Proposed mechanism for the selective formation of INT2a^{•-} or INT3b^{•-}.

of INT2b, and therefore, the route to INT3b is likely to proceed to avoid steric repulsion of the carboxylic acid with the olefin moiety (Fig. 2c).

Owing to the high electronegativity of the fluorine atom, HF typically exists as oligomers and readily undergoes self-ionization to form HF₂⁻. It also readily forms hydrate complexes upon exposure to a humid environment [17]. Consequently, producing a non-naturally occurring form of HF poses a synthetic challenge. Thus, we attempted HF insertion into 3b (Fig. 3a). Powdery H₂O@3b (H₂O: 39%) was dissolved in ODCB in a sealed Teflon vessel. An excess of hydrogen fluoride pyridine complex was added, and the resulting solution was stirred at 22 °C for 24 h and 0 °C for 24 h. After the reaction, the crude mixture was treated with saturated Na₂CO₃ and extracted with CS₂. Chromatographic purification yielded the sole product

without considerable decomposition of 3b. The ¹H NMR spectra exhibited a singlet signal at δ = 10.09 ppm corresponding to H₂O@3b (Fig. 3b), indicating that the pre-encapsulated H₂O molecule remains encapsulated with an unchanged occupation level of 39% under both conditions at 22 °C and 0 °C. We also observed a doublet signal at δ = 7.53 ppm, which can be assigned to HF@3b. The coupling constant was measured to be J_{HF} = 508 Hz, which is comparable to those reported for HF in fullerene derivatives [18–20]. The ¹⁹F NMR signal of HF@3b was detected at −225.76 ppm as a doublet signal. The encapsulation ratio of HF was determined to be 6% and 18% for the reactions performed at 22 °C and 0 °C, respectively, while the encapsulation ratio of H₂O remained unchanged. This is in contrast to the report by Gan and coworkers, who demonstrated the release of the encapsulated H₂O molecule mediated by HF [21]. Because 39% of

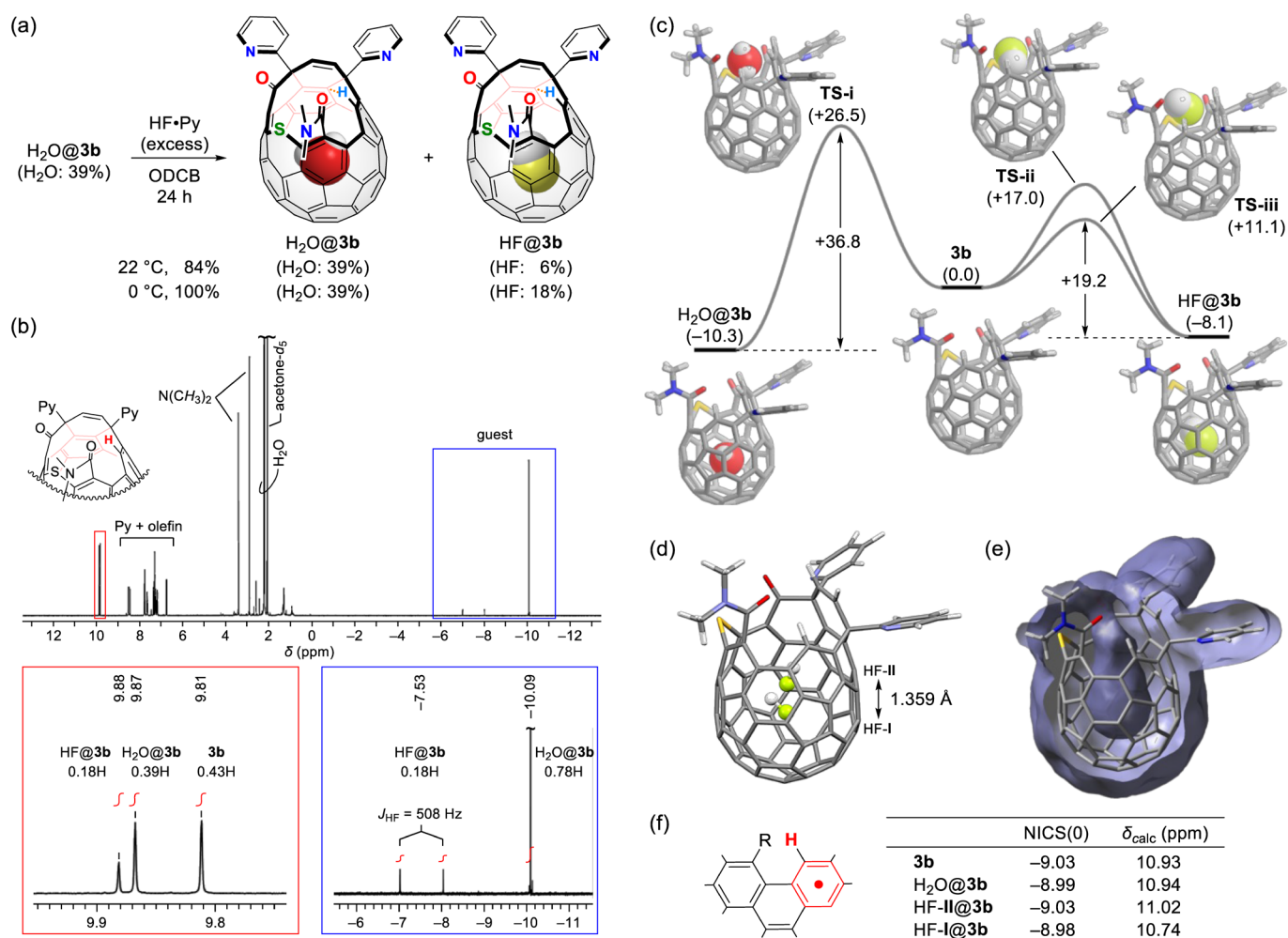


Fig. 3 (a) HF insertion into **3b**. (b) ¹H NMR spectra (500 MHz, acetone-*d*₆/CS₂ (1 : 5)) of X@**3b** (X=HF, 18%; H₂O, 39%; empty, 43%). (c) Guest insertion mechanism (B3LYP-D3/6-31G(d)). ΔG values are given in kcal/mol at 298 K. (d) Structural overlay of HF-I@**3b** and HF-II@**3b** (B3LYP-D3/6-31G(d,p)). (e) van der Waals surface plot of **3b**. (f) NICS(0) (HF/6-311G(d,p)/B3LYP-D3/6-31G(d,p)) and simulated proton chemical shifts (GIAO-B3LYP-D3/6-311G(d,p)/B3LYP-D3/6-31G(d,p)) for **3b**, H₂O@**3b**, HF-I@**3b**, and HF-II@**3b**.

3b was already occupied by water, the net encapsulation ratio of HF was estimated to be 10% and 31% at each temperature. The lower encapsulation ratio of HF at a higher temperature suggests that HF readily escapes even after encapsulation. Therefore, these values reflect the thermal equilibrium in the reaction system at the applied temperatures. In fact, at room temperature, the complete release of HF from HF@**3b** (18%) was confirmed a few days after isolation as a mixture with **3b** (43%) and H₂O@**3b** (39%). According to theoretical calculations (Fig. 3c), the release barrier of H₂O from **3b** is ΔG[‡] +36.8 kcal/mol (TS-i), which is too high for the process to occur. This observation aligns well with the experimental finding that the water occupation level remains unchanged during the reaction. Theoretical calculations revealed two possible routes for HF insertion into **3b** with low activation barriers of +17.0 (TS-ii) and +11.1 kcal/mol (TS-iii). The lower activation barrier for TS-iii is attributed to the assistance provided by the intermolecular hydrogen bonding between the inserting HF and the amide moiety on the aperture. Unlike water in **3b**, HF can be released with a barrier of only +19.2 kcal/mol, which is again con-

sistent with the experimental observations.

Interestingly, **3b** contains an aromatic proton of a benzene ring in a bay region. The corresponding ¹H NMR signal serves as a valuable indicator of fullerene aromaticity. In the case of **3b**, this signal appears at δ 9.81 ppm (acetone-*d*₆/CS₂ (1 : 5)) (Fig. 3b), which is more deshielded than that of phenanthrene (δ 8.84 ppm, acetone-*d*₆) [22], indicating the electron-deficient nature of the fullerene cage. For H₂O@**3b**, this signal is slightly downfield-shifted to δ 9.87 ppm. Such a change in chemical shift is expected because encapsulation can lead to a slight deformation of the fullerene cage, and larger guests tend to induce greater changes [23]. Unexpectedly, the aromatic proton signal of HF@**3b** was detected at δ 9.88 ppm. This observation deviates from the intuitive prediction based on guest size, as HF is smaller than H₂O. Notably, in previous studies on HF in fullerene hosts [18–20], no considerable deviation in the ¹H signals of the addends between HF@hosts and empty hosts was observed owing to the small size of HF. Similarly, in this study, the change in chemical shifts of the addends (including protons in the olefin and

pyridyl substituents) is minimal. In contrast, a considerable deviation was observed only for protons directly attached to the [60]fullerene cage (Fig. S4). During the detailed computational analysis, we found that translational motion of HF in the fullerene cage was possible. Structural optimization suggested two orientations along the *z*-axis pointing toward the aperture (Fig. 3d). This type of dual positioning was not observed for H₂O@3b. The smaller size of HF may enable it to adopt an orientation closer to the aperture, where the void diameter is considerably narrower, as confirmed by the van der Waals surface plot (Fig. 3e). The calculated translational displacement was 1.359 Å, which is rather larger than water displacement in open-[60]fullerene with a large aperture (0.87(6) Å [24]) and closed [70]fullerene derivatives (0.70(2) [25] and 0.66(3) Å [26]).

To elucidate the discrepancy in guest-dependent chemical shifts, we calculated the nucleus-independent chemical shifts (NICS(0)) for the benzene ring and the chemical shifts of the proton in the benzene ring (Fig. 4a). The NICS(0) values for all structures were comparable, indicating that local aromaticity does not considerably contribute to the chemical shift. Although the simulated proton chemical shifts were slightly overestimated, the downfield shift for H₂O@3b ($\delta_{\text{calc}} + 10.94$ ppm) relative to 3b ($\delta_{\text{calc}} + 10.93$ ppm) was reproduced. However, an upfield shift was predicted for HF-I@3b ($\delta_{\text{calc}} + 10.74$ ppm), which should be canceled out by the large downfield shift predicted for HF-II@3b ($\delta_{\text{calc}} + 11.02$ ppm). The two structures with different HF positions have nearly identical Gibbs energies, with the latter being only slightly less stable than the former by $\Delta G + 0.12$ kcal/mol at 298 K. Assuming a Boltzmann distribution, this Gibbs energy difference corresponds to HF-I@3b : HF-II@3b = 55 : 45. Therefore, the HF-II@3b structure would contribute considerably to the unusually large shift of the proton signal.

3. Conclusion

We synthesized small apertures with a 14-membered ring on the C₆₀ cage (2 and 3) via reductive decarbonylation of 1, which possesses a 13-membered-ring aperture. By substituting an imine functionality on the aperture with an olefin analog, the selectivity between 2 and 3 was reversed. 2a (35% isolated yield) became the major product over 3a (3%), while 2b (4%) was obtained as the minor product along with 3b (68%). This reversed selectivity may be attributed to the stabilization of the transition state for converting INT1a⁺ into INT2a⁺, where the hydroxy group forms intramolecular hydrogen bonds with the imine moiety. During the reaction, these host materials spontaneously incorporate a water molecule at a level of 22–78%. Using H₂O@3b (H₂O: 39%), we attempted HF inclusion at 0 °C for 24 h, achieving 18% encapsulation of HF without any change in the water content. The proton signals of the addends, especially at the benzene ring in 3b, were affected by the guests, with the smaller HF guest inducing a larger change in the chemical shift compared to the

larger H₂O guest. Theoretical calculations suggest that HF undergoes translational motion in the cavity of 3b, with a displacement of 1.359 Å. The upper disposition of HF would contribute to the larger shift owing to the closer distance to the benzene ring on the aperture.

Acknowledgements

Financial support was partially provided by the JSPS KAKENHI Grant Number JP23H01784 and JP23K17916, Advanced Technology Institute Research Grants 2023, ISHIZUE 2024 of Kyoto University, and JACI Prize for Encouraging Young Researcher. The NMR measurements were partly supported by the Joint Usage/Research Center (JURC) at the ICR, Kyoto University.

References

- [1] G.C. Vougioukalakis, M.M. Roubelakis, M. Orfanopoulos, Open-cage fullerenes: towards the construction of nanosized molecular containers, *Chem. Soc. Rev.* 39 (2010) 817–844.
- [2] L. Shi, L. Gan, Open-cage fullerenes as tailor-made container for a single water molecule, *J. Phys. Org. Chem.* 26 (2013) 766–772.
- [3] Y. Hashikawa, Y. Murata, Water in Fullerenes, *Bull. Chem. Soc. Jpn.* 96 (2023) 943–967.
- [4] M. Murata, Y. Murata, K. Komatsu, Surgery of fullerenes, *Chem. Commun.* 2008 (2008) 6083–6094.
- [5] Y. Hashikawa, T. Fushino, Y. Murata, Double-Holed Fullerenes, *J. Am. Chem. Soc.* 142 (2020) 20572–20576.
- [6] G. Schick, T. Jarrosson, Y. Rubin, Formation of an Effective Opening within the Fullerene Core of C₆₀ by an Unusual Reaction Sequence, *Angew. Chem. Int. Ed.* 38 (1999) 2360–2363.
- [7] Y. Rubin, T. Jarrosson, G.-W. Wang, M.D. Bartberger, K.N. Houk, G. Schick, M. Saunders, R.J. Cross, Insertion of Helium and Molecular Hydrogen Through the Orifice of an Open Fullerene, *Angew. Chem. Int. Ed.* 40 (2001) 1543–1546.
- [8] K. Kurotobi, Y. Murata, A Single Molecule of Water Encapsulated in Fullerene C₆₀, *Science* 333 (2011) 613–616.
- [9] Y. Hashikawa, K. Kizaki, T. Hirose, Y. Murata, An Orifice Design: Water Insertion into C₆₀, *RSC Adv.* 10 (2020) 40406–40410.
- [10] Y. Hashikawa, K. Kizaki, Y. Murata, Pressure-induced annulative orifice closure of a cage-opened C₆₀ derivative, *Chem. Commun.* 57 (2021) 5322–5325.
- [11] Y. Hashikawa, Y. Murata, Water-Mediated Thermal Rearrangement of a Cage-Opened C₆₀ Derivative, *ChemPlusChem* 86 (2021) 1559–1562.
- [12] Y. Hashikawa, S. Sadai, S. Okamoto, Y. Murata, Near-Infrared-Absorbing Chiral Open [60]Fullerenes, *Angew. Chem. Int. Ed.* 62 (2023) e202215380.
- [13] J.C. Hummelen, M. Prato, F. Wudl, There Is a Hole in My Bucky, *J. Am. Chem. Soc.* 117 (1995) 7003–7004.
- [14] Y. Hashikawa, M. Murata, A. Wakamiya, Y. Murata, Synthesis of Open-Cage Ketolactam Derivatives of Fullerene C₆₀ Encapsulating a Hydrogen Molecule, *Org. Lett.* 16 (2014) 2970–2973.
- [15] Y. Hashikawa, M. Murata, A. Wakamiya, Y. Murata, Synthesis and Properties of Endohedral Aza[60]fullerenes: H₂O@C₅₉N and H₂@C₅₉N as Their Dimers and Monomers, *J. Am. Chem. Soc.* 138 (2016) 4096–4104.
- [16] Y. Hashikawa, S. Sadai, Y. Murata, Reductive Decarbonylation of a Cage-Opened C₆₀ Derivative, *Org. Lett.* 23 (2021) 9495–9499.
- [17] J.H. Simons, Hydrogen Fluoride and its Solutions, *Chem. Rev.* 8 (1931) 213–235.

- [18] A. Krachmalnicoff, R. Bounds, S. Mamone, M.H. Levitt, M. Carravetta, R.J. Whitby, Synthesis and characterisation of an open-cage fullerene encapsulating hydrogen fluoride, *Chem. Commun.* 51 (2015) 4993–4996.
- [19] A. Krachmalnicoff, R. Bounds, S. Mamone, S. Alom, M. Concistrè, B. Meier, K. Kouřil, M.E. Light, M.R. Johnson, S. Rols, A.J. Horsewill, A. Shugai, U. Nagel, T. Rõdm, M. Carravetta, M.H. Levitt, R.J. Whitby, The dipolar endofullerene HF@C₆₀, *Nat. Chem.* 8 (2016) 953–957.
- [20] R. Zhang, M. Murata, A. Wakamiya, T. Shimoaka, T. Hasegawa, Y. Murata, Isolation of the simplest hydrated acid, *Sci. Adv.* 3 (2017) e1602833.
- [21] L. Xu, H. Ren, S. Liang, J. Sun, Y. Liu, L. Gan, Release of the Water Molecule Encapsulated Inside an Open-Cage Fullerene through Hydrogen Bonding Mediated by Hydrogen Fluoride, *Chemistry* 21 (2015) 13539–13543.
- [22] E.E. Brotherton, D.H.H. Chan, S.P. Armes, R. Janani, C. Sammon, J.L. Wills, J.D. Tandy, M.J. Burchell, P.J. Wozniakiewicz, L.S. Alesbrook, M. Tabata, Synthesis of Phenanthrene/Pyrene Hybrid Microparticles: Useful Synthetic Mimics for Polycyclic Aromatic Hydrocarbon-Based Cosmic Dust, *J. Am. Chem. Soc.* 146 (2024) 20802–20813.
- [23] G. Huang, Y. Ide, Y. Hashikawa, T. Hirose, Y. Murata, CH₃CN@open-C₆₀: An Effective Inner-Space Modification and Isotope Effect inside a Nano-Sized Flask, *Chem. Eur. J.* 29 (2023) e202301161.
- [24] Y. Hashikawa, S. Hasegawa, Y. Murata, A Single but Hydrogen-Bonded Water Molecule Confined in an Anisotropic Subnanospace, *Chem. Commun.* 54 (2018) 13686–13689.
- [25] R. Zhang, M. Murata, T. Aharen, A. Wakamiya, T. Shimoaka, T. Hasegawa, Y. Murata, Synthesis of a distinct water dimer inside fullerene C₇₀, *Nat. Chem.* 8 (2016) 435–441.
- [26] S. Zhang, Y. Hashikawa, Y. Murata, Cage-Expansion of Fullerenes, *J. Am. Chem. Soc.* 143 (2021) 12450–12454.